In-Plane Retardation of Collective Expansion in Au + Au Collisions

S. Wang,[2] M. A. Lisa,[1] S. Albergo,[6] F. Bieser,[1] F. P. Brady,[4] Z. Caccia,[6] D. A. Cebra,[4] A. D. Chacon,[5] J. L. Chance,[4] Y. Choi,[3] S. Costa,[6] J. B. Elliott,[3] M. L. Gilkes,[3] J. A. Hauger,[3] A. S. Hirsch,[3] E. L. Hjort,[3] A. Insolia,[6] M. Justice,[2] D. Keane,[2] J. Kintner,[4] V. Lindenstruth,[1] H. Liu,[2] H. S. Matis,[1] M. McMahan,[1] C. McParland,[1] D. L. Olson,[1] M. D. Partlan,[4,1] N. T. Porile,[3] R. Potenza,[6] G. Rai,[1] J. Rasmussen,[1] H. G. Ritter,[1] J. Romanski,[6] J. L. Romero,[4] G. V. Russo,[6] R. P. Scharenberg,[3] A. Scott,[2] Y. Shao,[2] B. K. Srivastava,[3] T. J. M. Symons,[1] M. L. Tincknell,[3] C. Tuvè,[6] P. G. Warren,[3] D. Weerasundara,[2] H. H. Wieman,[1] and K. L. Wolf[5]

(EOS Collaboration)

[1]*Lawrence Berkeley National Laboratory, Berkeley, California 94720*
[2]*Kent State University, Kent, Ohio 44242*
[3]*Purdue University, West Lafayette, Indiana 47907*
[4]*University of California, Davis, California 95616*
[5]*Texas A&M University, College Station, Texas 77843*
[6]*Università di Catania and Istituto Nazionale di Fisica Nucleare Sezione di Catania, 95129 Catania, Italy*
(Received 13 October 1995)

Using charged-particle-exclusive measurements of Au + Au collisions in the Bevalac's EOS time projection chamber, we demonstrate the advantages of an alternative representation of the squeeze-out phenomenon where the speed of collective expansion is slowest in the plane of the reaction, and is modulated sinusoidally according to fragment azimuth relative to this plane. This simpler representation facilitates a highly comprehensive description of light fragment spectra and the three main categories of collective motion: sideward flow, squeeze-out, and radial expansion. [S0031-9007(96)00270-0]

PACS numbers: 25.75.Ld, 25.70.Pq

In order to probe the early, high-density stage of a nucleus-nucleus collision, it is necessary to focus on observables that become established during this early phase, and then remain almost constant as the system evolves towards its final state. Hydrodynamic [1–3] and nuclear transport [4–6] models indicate that in collisions at nonzero impact parameter, fluidlike sideward deflection of fragments ("sideward flow") has this desired property. These models also support the interpretation that sideward flow provides a useful relative measure of the peak nuclear pressure generated in the collision. The "squeeze-out" phenomenon [7–10], a preferential emission of fragments perpendicular rather than parallel to the reaction plane, is reported to surpass [11] or at least match [12] sideward flow in this regard. The fragments emitted from heavy ion collisions are inferred to undergo another type of collective motion—an omnidirectional expansion ("radial flow") [13–17].

There have been earlier measurements of single-particle spectra and of aspects of the three types of collective motion cited above, in some cases as a function of a centrality observable and in some cases for different fragment species, but these results have been derived from a variety of detectors and separate analyses. In this Letter, we (a) introduce a more complete yet simpler and more intuitive description of squeeze-out, (b) use a nuclear transport model to argue that the in-plane retardation of collective expansion is sensitive to nuclear incompressibility, and (c) present a unified and comprehensive description of collective motion and single-particle spectra for light fragments, with small and well-quantified detector distortions.

This Letter is based on Au + Au data from the EOS time projection chamber (TPC) at Lawrence Berkeley National Laboratory. This TPC is the principal subsystem of the EOS detector; it has rectangular geometry and operates in a 1.3 T magnetic field. Details about the detector and its performance can be found elsewhere [18–20]. Following the convention introduced by the Plastic Ball group, we characterize the centrality of collisions in terms of baryonic fragment multiplicity M as a fraction of $M_{\max}$, where $M_{\max}$ is a value near the upper limit of the M spectrum where the height of the distribution has fallen to half its plateau value [21]. Mul1 through Mul4 denote the four intervals of M with upper boundaries at 0.25, 0.5, 0.75, and 1.0 times $M_{\max}$, respectively, and Mul5 denotes $M > M_{\max}$. The quantum molecular dynamics (QMD) [6,22] model indicates that Mul3, Mul4, and Mul5 correspond to mean impact parameters of 6.1, 4.3, and 2.3 fm, respectively. For our study of collisions at constant beam energy, we analyze data at $E_{\text{beam}} = 0.6A$ GeV, where a relatively large sample of events (31 000 with Mul3 and above) has been processed.

Important advantages of the EOS TPC are its good particle identification [19], the fact that it can be simulated with good accuracy, and its seamless acceptance that is consistently high in the forward half of rapidity space. Using the projectile-target symmetry of the Au + Au system, the

 © 1996 The American Physical Society

backward half of rapidity space is replaced by a reflection of the forward half. Using various event generators, we have compared the observables under investigation before and after filtering through a detailed GEANT-based simulation of the TPC. We infer that detector distortions are no larger than the symbol sizes or error bars in all figures.

In establishing $\Phi_i = \phi_i - \phi_R$, the azimuthal angle of fragment i relative to the estimated reaction plane, we use the vector $\mathbf{Q}_i = \sum_{j\neq i}^{M} w(y_j)\mathbf{p}_j^{\perp}$ to define ϕ_R [23], where j runs over all baryonic fragments, y_j is center-of-mass rapidity for fragment j divided by the projectile rapidity, and $\mathbf{p}^{\perp}$ is momentum in the plane perpendicular to the projectile direction. We use the weighting factor $w(y_j) = y_j/\max(|y_j|, 0.8)$, which results in a smaller reaction plane dispersion than the standard weighting prescription [23].

The squeeze-out anisotropy is known to be most readily detected at midrapidity [8,9], and is enhanced when observed in a coordinate system in which the sideward flow effect is canceled by applying a CM frame rotation through an angle Θ in the plane of the reaction [9,10,24]. In a picture where the event shape in momentum space is represented by an ellipsoid whose major axis is tilted an angle Θ from the beam direction (z), the rotated z axis lies along the major axis of the ellipsoid. In the present work, we rotate all events in the same multiplicity interval through the same angle, and determine Θ by maximizing squeeze-out. However, we find that the rotation angle for minimum flow (determining flow by any one of a variety of methods [23,25,26]) coincides within uncertainties with maximum squeeze-out. We use primed symbols to denote quantities evaluated in the rotated coordinate system. For simplicity, we present all measurements in the estimated reaction plane; rms dispersion angles [23] in determining this plane are 22°, 18°, and 21° for Mul3, Mul4, and Mul5, respectively, at $E_{\text{beam}} = 0.6A$ GeV.

Figure 1 presents results for $0.6A$ GeV Au + Au collisions, showing spectra of transverse mass $m'_\perp = (p'^2_\perp + m^2)^{1/2}$ for deuterons emitted near center-of-mass rapidity ($|y'| < 0.4$). The open circles label out-of-plane fragments ($\Phi' = 90°$ or $270° \pm 18°$) and the solid circles are for in-plane fragments ($\Phi' = 0°$ or $180° \pm 18°$). Squeeze-out manifests itself as an increasing divergence between these two spectra with increasing $m'_\perp$.

If fragments are emitted from a thermalized spherical shell at temperature T, expanding with velocity β, the expected distribution in $m_\perp$ and y has the form [13,17]

$$\frac{dN}{m_\perp^2\, dm_\perp\, dy} = N_0 \cosh y \left[\frac{\sinh\alpha}{\alpha}(\gamma + T_r) - T_r \cosh\alpha\right] \times \exp(-\gamma/T_r), \quad (1)$$

where $T_r = T/m_\perp \cosh y$, $\alpha = \beta\gamma p/T$, and $\gamma = 1/\sqrt{1-\beta^2}$. It has already been demonstrated that midrapidity spectra observed in the EOS TPC in the unrotated frame are well described by this functional form when averaged over all azimuths [17]. The solid curves

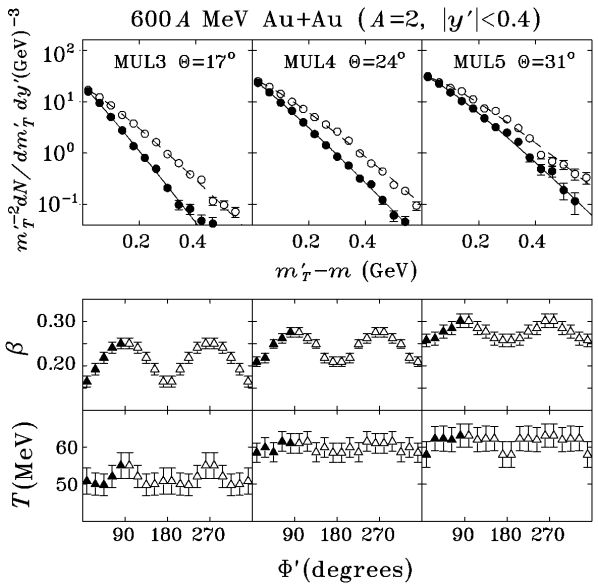

FIG. 1. The upper panels show deuteron transverse mass spectra at $\Phi' = 0$ (solid circles) and $\Phi' = 90°$ (open circles), in units of tracks/event/(GeV)^3/unit of y'. The curves are fits using Eq. (1). The lower panels present best-fit Eq. (1) parameters over the complete range of Φ'. The open symbols were generated by reflection of the closed symbols.

in Fig. 1 show the χ^2-minimized fit of Eq. (1) to the in-plane spectra, and the dashed curves show the same for the out-of-plane spectra. We constrain the area under each fitted curve to match the data, and T and β are the only free parameters. As expected *a priori,* the fitted curves for the in-plane and out-of-plane spectra are the same within errors at $p'_\perp = 0$.

The lower panels of Fig. 1 present the fitted T and β values as a function of Φ'. If we plot over the range 0° to 180°, results are consistently symmetric about $\Phi' = 90°$ within statistical uncertainties. Therefore, we choose to reflect all fragments into five Φ' bins spanning a single quadrant. Since it is customary to display squeeze-out over 360° of azimuth, our five independent fit points have been reflected 3 times to generate the data in the lower panels of Fig. 1. The data in Fig. 1 are consistent with the expansion velocity having the form $\beta(\Phi') = \beta_0 - \Delta\beta \cos 2\Phi'$, and with T being constant as function of Φ'. Values of χ^2 per degree of freedom (ν) for the fits are typically 0.8. When we assume constant β and a sinusoidal modulation of the parameter T, the χ^2/ν increases by a factor of about 3 for in-plane spectra, and typically increases to about 10 for out-of-plane spectra. In all remaining fits to $m_\perp$ spectra, we constrain both the vertical axis intercept and T to be independent of Φ', and we determine $\beta(\Phi')$ by minimizing χ^2. Adjusting β so that the $m'_\perp$ spectra have the same integrals as the data yields the same results within statistical errors.

Squeeze-out is normally characterized in terms of the $\cos 2\Phi'$ component in the number or total energy of fragments as a function of Φ'. Since this component increases markedly with $m_\perp$, a complete characterization of

squeeze-out in this framework would involve many separate anisotropy measurements. The most detailed squeeze-out analysis to date [10] was confined to the low end of the $p_\perp$ acceptance. In contrast, the amplitude $\Delta\beta$ of the sinusoidal modulation of the expansion velocity is a single parameter that constitutes a new and simpler description of the squeeze-out phenomenon over the entire $m'_\perp$ range. In this simpler picture of squeeze-out, out-of-plane expansion proceeds relatively unhindered, whereas in the reaction plane, the additional rescattering causes a slower collective expansion.

It has been known since the 1970s that the observed invariant momentum-space density ρ_A for fragments with mass number A and momentum $A\mathbf{p}$ closely follows the Ath power of the observed proton density ρ_1^A at momentum $\mathbf{p}$—a result that is consistent with composite fragment formation through coalescence [27]. This momentum-space power law also elucidates the observed increase in sideward flow per nucleon with fragment mass [28]. Assuming Eq. (1), the momentum-space power law requires the slope parameter T to be the same for all A if $\beta = 0$, but otherwise, it results in both β and T varying with A. To investigate the mass dependence of $\beta(\Phi')$, Fig. 2 presents the fitted in-plane and out-of-plane β for fragments of mass A, and compares these with various fitted β values based on applying the power law with exponent A/A^* to spectra for mass $A^* < A$. In Fig. 2, we constrain T for a spectrum derived from applying the power law to data for mass A^* to be the same as for the species with larger mass A; without this constraint, fitted β and T values change little, but uncertainties become larger. The reported departures from power law behavior at low $p_\perp$ [28] are not prominent on a logarithmic scale such as in Fig. 1, and are neglected in this analysis. The results in Fig. 2 demonstrate that the variation of the mean radial expansion velocity β_0 with fragment mass and the increase in squeeze-out $\Delta\beta$ with fragment mass are both consistent with the momentum-space power law for $A^* = 2$ and 3. Minor departures from the power law at the 2σ level are apparent for spectra based on the proton momentum-space density ρ_1 ($A^* = 1$); however, proton spectra are known to be distorted by baryonic and nuclear resonance decays [17]. These considerations prompted our choice of deuterons for the various spectra presented in Figs. 1 and 3.

The generally good adherence to the power law means that transport codes of the Boltzmann-Uehling-Uhlenbeck type [4,5], which determine only the evolution of one-body phase space and generally do not explicitly treat composite fragments, can be compared readily with our data if the normalization of spectra for the different fragment types is known. These normalizations are provided in Table I.

Next, we turn to Fig. 3 and the rapidity (y') dependence of Θ (the angle between the z and z' axes), β_0 and $\Delta\beta$. The parameter T is consistent with being constant over the analyzed y' region, and is so constrained in Fig. 3. The uppermost row of panels demonstrates that Θ is not independent of y' (as implicitly assumed in analyses based on the sphericity tensor [25], which fits an ellipsoid to the event shape) but instead peaks at midrapidity. In the unrotated coordinate system, sideward flow effectively obscures squeeze-out except at midrapidity. However, Fig. 3 reveals no decrease in squeeze-out away from midrapidity, in qualitative agreement with an earlier analysis [10]. The curves in Fig. 3 show quantum molecular dynamics [6,22] transport calculations after processing through the detector simulation chain. The dashed (dotted) curves are for a stiff (soft) momentum-dependent equation of state. We infer

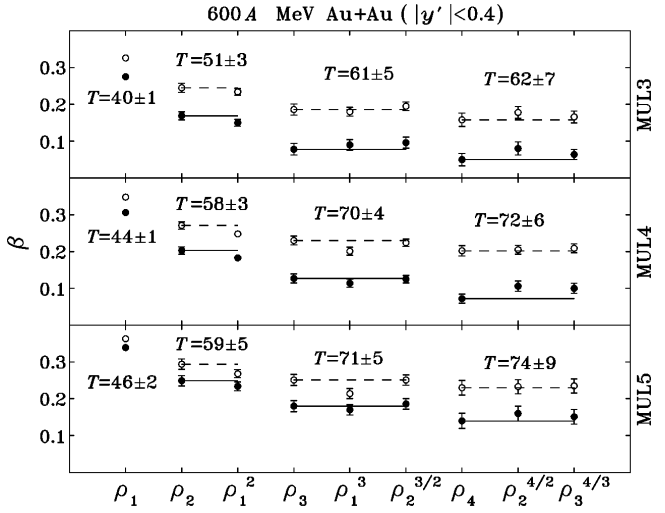

FIG. 2. Fitted β values at $\Phi' = 0$ (solid circles) and $\Phi' = 90°$ (open circles); on the horizontal axis, the notation ρ_A signifies results for fragments of mass A, while $\rho_{A^*}^p$ signifies that the momentum-space density for fragment A^* was raised to the power p and then the fit by Eq. (1) was performed. The horizontal lines serve only to guide the eye and are centered on the points for ρ_A.

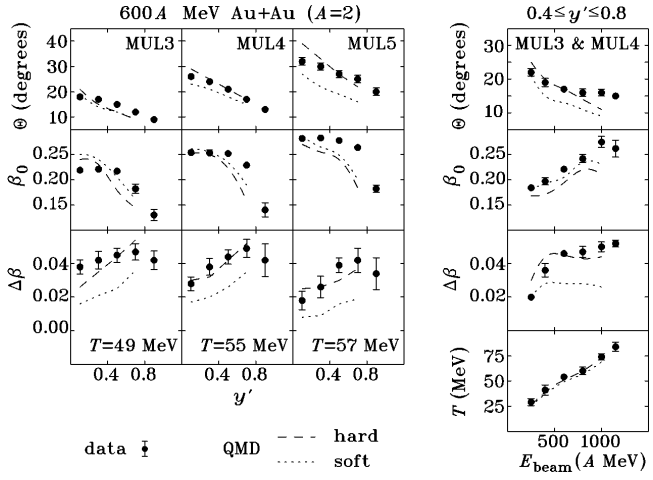

FIG. 3. The y' dependence of three observables which describe $m_\perp$ spectra, reflecting information about sideward flow, mean expansion velocity, and squeeze-out in three multiplicity gates; in conjunction with data in Table I, spectra for light fragment species other than $A = 2$ can be inferred. The right-hand set of panels presents excitation functions for the same three quantities and for the parameter T.

TABLE I. Fitted values of Eq. (1) at $p'_\perp = 0$ for light fragments in 0.6A GeV Au + Au collisions. The units are tracks/event/(GeV)^3/unit of y', and fitting uncertainties range from 1% to 4%.

	Mul3				Mul4				Mul5			
y'	ρ_1	ρ_2	ρ_3	ρ_4	ρ_1	ρ_2	ρ_3	ρ_4	ρ_1	ρ_2	ρ_3	ρ_4
0.1	116	18.1	6.2	1.0	166	27.0	9.6	2.0	226	33.6	12.0	2.4
0.3	128	19.6	8.4	1.6	154	27.2	11.0	2.4	212	33.2	11.8	2.4
0.5	158	24.2	10.6	5.0	190	30.2	6.6	5.6	210	31.6	11.2	4.8
0.7	232	35.2	17.4	9.6	230	37.2	8.4	6.8	228	33.0	12.4	2.8
0.9	264	39.6	20.2	15.6	244	38.8	9.6	9.2	226	29.8	11.4	3.0

that measurements of azimuth-averaged expansion velocity, β_0, offer minimal sensitivity to incompressibility, as reported previously [17,29], while the in-plane retardation of collective expansion, $\Delta\beta$, shows much greater promise as a probe of the nuclear equation of state.

Finally, the right-hand set of panels in Fig. 3 presents Θ, β_0, $\Delta\beta$, and T at beam energies of 0.25, 0.4, 0.6, 0.8, 1.0, and 1.15A GeV, for $0.4 \leq y' \leq 0.8$. This rapidity gate has been chosen so as to minimize detector distortions, which tend to increase below $y' \sim 0.4$ at the lower beam energies and above $y' \sim 0.8$ at the higher beam energies. The Θ, T, and β_0 excitation functions have similar magnitudes and trends as previous measurements of related observables [17,30]. Our results are consistent with the in-plane retardation signal $\Delta\beta$ remaining constant or increasing slightly up to the maximum energy. The QMD comparisons do not show a level of agreement with the data that justifies drawing inferences about nuclear incompressibility.

In summary, this work introduces a simple yet complete characterization of squeeze-out, leading to its interpretation as an in-plane retardation of collective expansion. Our measurements offer promise as a probe of the nuclear equation of state, and also facilitate a comprehensive and coordinated description of the single-particle spectra and the three categories of collective motion, for light fragment species in three multiplicity intervals spanning intermediate and central collisions of 0.6A GeV Au + Au. Information has also been presented for five other beam energies in the range 0.25A to 1.15A GeV; noteworthy observations include a level or slightly increasing trend with beam energy, up to 1.15A GeV, in the in-plane retardation of collective expansion.

This work is supported in part by the U.S. Department of Energy under Contracts/Grants No. DE-AC03-76SF00098, No. DE-FG02-89ER40531, No. DE-FG02-88ER40408, No. DE-FG02-88ER40412, No. DE-FG05-88ER40437, and by the U.S. National Science Foundation under Grant No. PHY-9123301.

[1] G. F. Chapline *et al.*, Phys. Rev. D **8**, 4302 (1973).
[2] W. Scheid, H. Müller, and W. Greiner, Phys. Rev. Lett. **32**, 741 (1974).
[3] H. Stöcker, J. Maruhn, and W. Greiner, Z. Phys. A **293**, 173 (1979); Phys. Rev. Lett. **44**, 725 (1980).
[4] G. Bertsch, H. Kruse, and S. DasGupta, Phys. Rev. C **29**, 673 (1984).
[5] H. Kruse, B. V. Jacak, and H. Stöcker, Phys. Rev. Lett. **54**, 289 (1985).
[6] J. Aichelin and H. Stöcker, Phys. Lett. B **176**, 14 (1986).
[7] H. Stöcker *et al.*, Phys. Rev. C **25**, 1873 (1982).
[8] D. L'Hôte, in Proceedings of the 5th Gull Lake Nuclear Physics Conference, Hickory Corners, Michigan, 1988 (unpublished); J. Gosset *et al.*, in *The Nuclear Equation of State*, edited by W. Greiner and H. Stöcker, NATO ASI, Ser. A, Vol. B216 (Plenum, New York, 1989), p. 87.
[9] H. H. Gutbrod *et al.*, Phys. Lett. B **216**, 267 (1989).
[10] H. H. Gutbrod *et al.*, Phys. Rev. C **42**, 640 (1990).
[11] P. Danielewicz, Phys. Rev. C **51**, 716 (1995).
[12] C. Hartnack *et al.*, Nucl. Phys. **A538**, 53c (1992).
[13] P. J. Siemens and J. O. Rasmussen, Phys. Rev. Lett. **42**, 880 (1979).
[14] H. W. Barz *et al.*, Nucl. Phys. **A531**, 453 (1991).
[15] S. C. Jeong *et al.*, Phys. Rev. Lett. **72**, 3468 (1994).
[16] W. C. Hsi *et al.*, Phys. Rev. Lett. **73**, 3367 (1994).
[17] M. A. Lisa *et al.*, Phys. Rev. Lett. **75**, 2662 (1995).
[18] G. Rai *et al.*, IEEE Trans. Nucl. Sci. **37**, 56 (1990).
[19] E. Hjort *et al.*, in *Advances in Nuclear Dynamics*, edited by B. Back, W. Bauer, and J. Harris (World Scientific, Singapore, 1993), p. 63.
[20] M. L. Gilkes *et al.*, Phys. Rev. Lett. **73**, 1590 (1994).
[21] H.-Å. Gustafsson *et al.*, Phys. Rev. Lett. **52**, 1590 (1984).
[22] G. Peilert *et al.*, Phys. Rev. C **39**, 1402 (1989).
[23] P. Danielewicz and G. Odyniec, Phys. Lett. **157B**, 146 (1985).
[24] C. Hartnack *et al.*, Phys. Lett. B **336**, 131 (1994).
[25] M. Gyulassy, K. A. Frankel, and H. Stöcker, Phys. Lett. **110B**, 185 (1982); P. Danielewicz and M. Gyulassy, Phys. Lett. **129B**, 283 (1983).
[26] S. Wang *et al.*, Phys. Rev. C **44**, 1091 (1991).
[27] H. H. Gutbrod *et al.*, Phys. Rev. Lett. **37**, 667 (1976); M.-C. Lemaire *et al.*, Phys. Lett. **85B**, 38 (1979).
[28] S. Wang *et al.*, Phys. Rev. Lett. **74**, 2646 (1995).
[29] P. Danielewicz and Q. Pan, Phys. Rev. C **46**, 2002 (1992).
[30] H. G. Ritter *et al.*, Nucl. Phys. **A447**, 3c (1985).